Pak. J. Chem. 14(1-2): 42-48, 2024 Research Article
ISSN (Print): 2220-2625
ISSN (Online): 2222-307X DOI: 10.15228/2024.v14. i1-2,p05

Synthesis and Characterization of Layered Silicate Na-Magadiites and its Application in Pollution Control

[1]M. Yamin, [2]N. Rohman, & [3*]K. Ahmed

[1]Institute of Chemistry, University of Campinas, UNICAMP., Campinas, SP, Brazil

[2]Department of Chemistry, College of Science, Sultan Qaboos University, PO Box 36, Al-khoudh, Muscat PC 123, Oman[3]L. E. J. Nanotechnology Centre, H. E. J. Research Institute of Chemistry, International Centre for Chemical and Biological Sciences, University of Karachi, Karachi – 75270, Pakistan

Corresponding author email: khalid.ahmed@iccs.edu

Abstract

Advancements in several industrial fields contribute to environmental pollution, predominantly after using essential heavy metals, organic compounds (including pharmaceuticals and dyes), and gaseous emissions such as carbon dioxide (CO_2), often released into the environment without prior treatment. Consequently, it enriches the pollution of water resources and bacteria in the soil. Researchers are searching for cost-effective and innovative methods, including synthesizing harmless active compounds to minimize the toxic effects of discharged waste products. This article provides the synthesis and characterization of the Layered Silicate Na Magadiites (LSNaM.), which have a unique structure where each layer is interconnected with tetrahedra. The synthesized LSNaM is characterized by nitrogen adsorption, thermogravimetry, X-ray diffraction, and scanning electron microscopy, and it was applied to laboratory-prepared dye wastewater. Results showed that the LSNaM exhibited significantly higher adsorption capacities for the reactive active blue dye (RB) with slow adsorption kinetics, and equilibrium typically reached within 3 to 4 hours. Moreover, the data were best described by a pseudo-first-order kinetic model. Additionally, the impact of pH on the adsorption process was investigated at ambient temperature. The findings suggest that LSNaM has the potential to serve as an efficient and cost-effective material for removing organic contaminants, such as dyes and organic pharmaceutical waste discharged in soil and streams.

***Keywords*:** LSNaM, adsorption, reactive blue, cost-effective.

1. INTRODUCTION

Pollution due to organic contaminates is dangerous as it enhances chemical oxygen demand. Colouring materials (dyes; organic compounds) are widely used in colouring, including fabrics, plastics, and paper [1-3]. The coloured water, after primary use, is usually discharged into rivers and lakes without proper sand-safe treatment, which poses a severe environmental concern [4, 5]. Traditional methods of dye removal from wastewater, such as physicochemical and biological methods, have proven ineffective due to synthetic dyes' resistance to fading under various conditions. Silica-based materials have gained attention as promising candidates for dye adsorption because of their high surface area, tunable pores, and surface functionalization capabilities [6-8]. The mesoporous structure of silica-based materials provides a large surface area for effective contaminant adsorption.

Additionally, the surface functional groups of silica-based materials can be tailored to enhance their affinity towards specific organic molecules. Silica-based materials have successfully eliminated various dyes and pollutants from wastewater [9, 10]. Their versatility and effectiveness make them suitable for large-scale applications in industries where dye-containing wastewater is a significant issue. The adsorption of dyes on silica-based materials can occur through various mechanisms, including electrostatic interactions, hydrogen bonding, and π-π interactions [11,12]. These proposed mechanisms efficiently remove diverse dye molecules from colourant wastewater through adsorption, decomposition, or degradation [13,14]. Magadiite is widely examined and cited in the literature. It is a naturally occurring crystalline structure first discovered by Eugster in Lake Magadi, Kenya, in 1967. [15, 16]. A group of researcher found in their research and demonstrated the reactivity of layered sheets of the interlayer Si-OH/Si-O- groups offer several intriguing properties[17, 18].

Furthermore, modifying surface properties, primarily through incorporating metal or any charged species, has increased the scope of applications for these layered materials [6, 19]. Surface area and flakes-like structure, coupled with their cost-effectiveness and widespread availability, layered silicates have emerged as highly sought-after adsorbents. Isomorphic substitution within the layers introduces negative charges, typically balanced by cations in the interlayer. The substitution of silicon with metal ions leads to modifications in Na-magadiite properties [20, 21]; the tetrahedra structure of LSM showed attractive properties in contaminate removal through adsorption. The present investigation provides a novel method for synthesizing the Layered Silicate Na Magadiites to control dye wastewater (Reactive blue) discharged without proper treatment in freshwater resources. The study includes kinetics of adsorption studies to check the efficiency of the synthesized Layered Silicate Na Magadiites in managing dye (Reactive blue) wastewater.

2. MATERIALS AND METHODS

All reagents and solvents, including Silica gel (Merck), NaOH, and reactive blue (RB) (Sigma Aldrich), were analytical grades utilized in their as-received without further purification. Deionized water was used exclusively throughout the experiments.

2.1. Synthesis of LSNaM

Based on previous reports [6, 22], Magadiite was prepared via hydrothermal method. In summary, 3.4 g of NaOH was added in 76.0 g of distilled water, 12 g of silica gel, and stirred for 20 minutes. The resulting solution was put to hydrothermal treatment at 425 K for 20 to 72 hours. Subsequently, the solid product was filtered, washed, and dried.

2.2. Characterization LSNaM

Infrared (IR) spectra were acquired using a Bruker Equinox 55 spectrophotometer, covering a wavelength range from 4000 to 400 cm^{-1} with a resolution of 4 cm^{-1}. X-ray measurements were conducted using a Bruker XRD 7000 instrument, and Thermogravimetric analyses (TGA) were performed using a thermobalance 1090 B. Nitrogen adsorption/desorption isotherms were measured using a Quanta chrome NOVA 4200 instrument. SEM images were captured using a Jeol JSM 6360-LV microscope operating at 20 kV. Absorption studies of the dye before and after the reaction were investigated at a wavelength of 595 nm using a Shimadzu spectrophotometer Model Multi Spec TCC-1501-240A, and the pH was measured by the Seven Easy Meter Toledo pH meter.

2.3. Efficiency of the LSNaM

The efficiency of LSM. was monitored through Adsorption kinetics where organic compounds Adsorption of Reactive Blue (RB) (Fig. 1) was selected

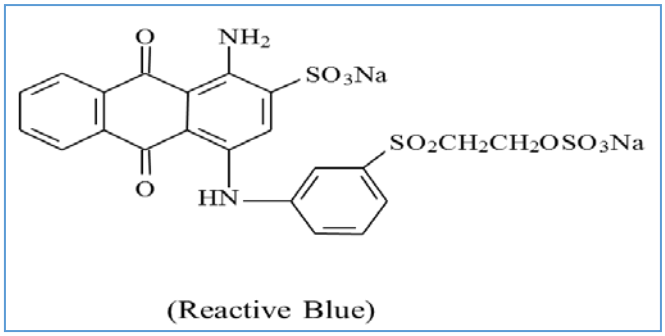

(Reactive Blue)

Figure 1: Structure formula of the Reactive Blue (RB) showing possible functional groups that may be involved in surface adsorption on LSNaM

Initial tests were conducted to assess the impact of the pH of the solution on the adsorption of RB; subsequently, under the optimal pH, the influence of time between the dye and adsorbent was investigated with the 4.0 mmol dm^{-3} of RB. Equilibrium studies were performed using all samples' optimal contact time, determined from the previous step. Solutions with varying concentrations, from 0.15 to 4.0 mmol $dm^{-3,}$ were employed to generate adsorption isotherms. The dye adsorbed on the fabricated silicate was quantified by filtering the dye-silicate dispersion and then by measuring the dye concentration using UV-Vis absorption spectroscopy. Utilizing data from the isotherm experiments, the equilibrium amount of dye adsorbed (qe), expressed in mmol of adsorbate per gram of adsorbent (mmol/ g), was calculated using Equation 1.

$$= \frac{(C_o - C_e)V}{} \quad (1)$$

where C_0 and C_e (mmol dm^{-3}) are the initial and equilibrium liquid-phase concentrations of the adsorbate, respectively, V is the solution volume (dm^3), and m is the adsorbent mass in gram [29]. In kinetic experiments, the amount of dye sorbed at any time t (q_t) in mmol g^{-1}, was calculated with Equation 2.

$$= \frac{(C_o - C_t)V}{} \quad (2)$$

C_t = concentration of dye at time t.

3. RESULTS AND DISCUSSION

3.1. Infrared spectroscopy

IR of LSNaM showed the bands in the 3640 to 3590 $cm^{-1,}$ which are similar to the earlier reports that the 3700-3000 cm-' region showed stretching vibrations of OH groups (vOH) from water molecules trapped within the silicate layers[23, 24]., while the bands at about 1660 to 1628 cm^{-1} (1670 and 1630 cm-') are due to bending vibrations (6HOH) of water molecules (Fig.2). The IR spectrum of LSNaM shows two OH stretching bands: a narrow band at higher frequency (3640 cm-') and a

broad one with a maximum at lower frequency (3590 cm-'), may be due to the isolated surface OH groups associated with layer structure and OH of water molecule. The band centred between 1400 to 500 cm^{-1} is attributed to the SiO_4 framework, while the band at 1075 cm^{-1} signifies asymmetric stretching and is assigned to the Si-O-Si and Si-O- groups (Fig.2). Additionally, symmetric stretching vibrations of Si-O-Si were detected within the range of 699 to 950 cm^{-1}[17].

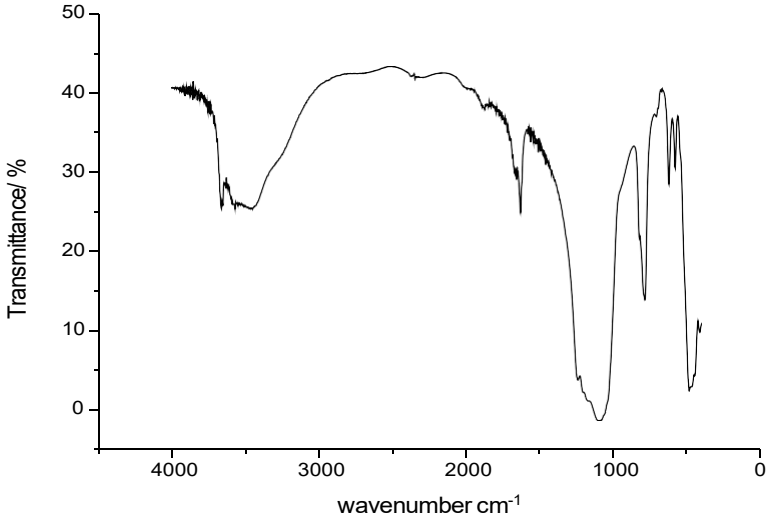

Figure 2. IR spectra of MLNaM [6]

3.2. X-ray diffraction

The interlayer region of the structure of Magadiite resembles channel-like, as shown in Fig. (3), displays the XRD pattern of magadiites, revealing a characteristic diffraction pattern at especially 5.6°, 17.1°, and 28.42°, corresponding to (hkl) lines with some presence of crystobalite [25] may be due to the formation of two types of layered silicates i) Na-magadiite and ii) Na-kenyaite.

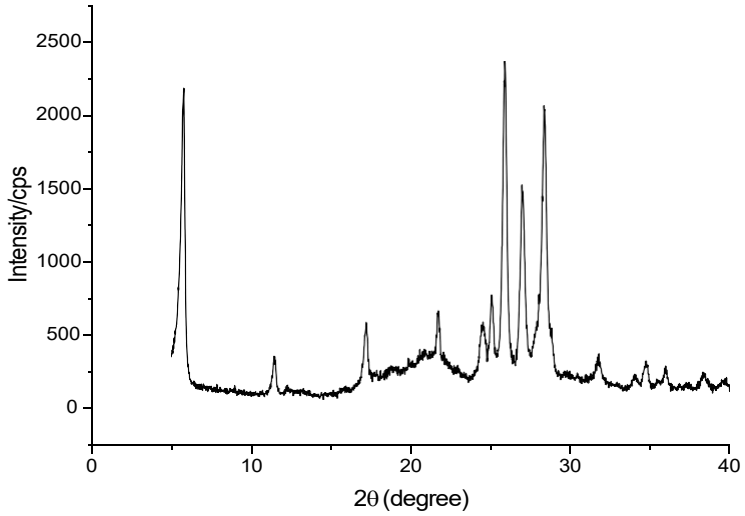

Figure 3. X-ray diffraction patterns of Na-mag [6].

3.3. Scanning electron microscopy

The SEM images of the LSNaM shown in Fig. (4) reveal a typical morphology characterized by layered rosette-shaped structures formed through the contact packing of well-defined plates with the size 5μ, as reported earlier [22, 25]. These images of Na Magadiite reveal the presence of both rosette and disk-shaped particles, confirming the coexistence of

crystalline and amorphous phases. The introduction of Na into the silicate framework decreased the crystallinity of Magadiite, consistent with observations from XRD data [25, 26].

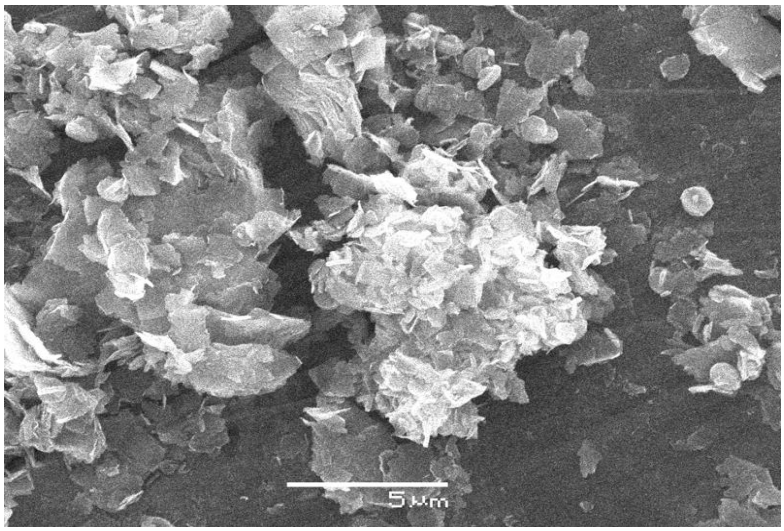

Figure 4: SEM image of Na-magadiite

The BET surface area of Magadiite was determined to be 28 m^2g^{-1}. This can tentatively be attributed to the presence of disk-shaped particles and the observed decrease in particle size as depicted in the SEM images (Fig.4).

3.4. Thermogravimetry

Fig. (5) depicts the thermogravimetric and derivative curves for Na-mag. Apart from the cristobalite contents, the curves for these synthesized LMNaS exhibit high similarity, differing mainly in the physisorbed water content. The synthesized Magadiite exhibited three mass losses occurring at specific temperatures: 350, 394, and 567 K for Na-magadiite. These losses are attributed to the elimination of water during the heating process, with molecules either hydrogen-bonded to other molecules or to the surface [25] as shown in Fig. (5). A comprehensive analysis of all MS curves revealed the presence of two temperature ranges, indicating the elimination of matter within the interlamellar cavity or possessing two distinct water sorption sites, with one range observed at 330 to 410 K and the other at 550 to 650 K [24, 27, 28].

Regarding the second step of mass loss, another distinct interval between 550 to 630 K can be observed, indicating the condensation of lamellar silanols and the subsequent elimination of additional water molecules. The total amount of water released was 9.5, 15.0, and 15.0 for Na-magadiite.

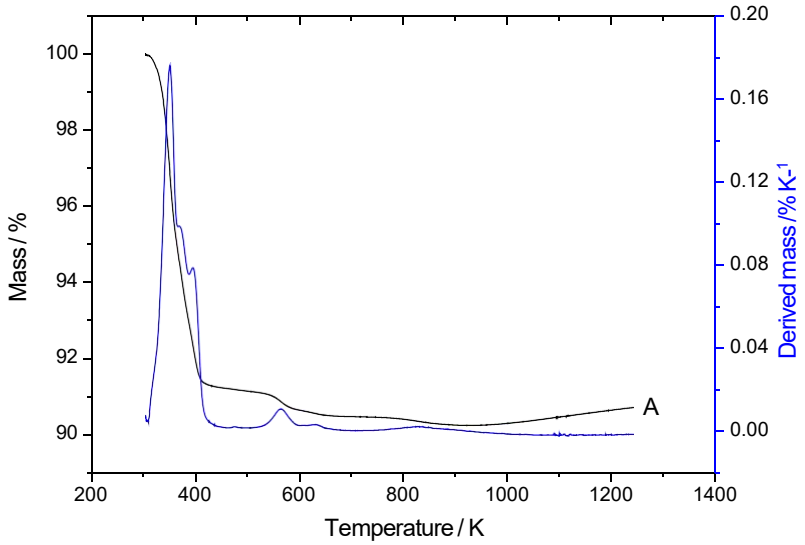

Figure 5. Thermogravimetric and derivative curves of LSNaM.

3.5. LSNaM efficiency

The efficiency of the dye adsorption process is significantly influenced by the structure of the adsorbent and adsorbate and the dissociation of the adsorbate, which leads to the generation of neutral, positive, or negative charges. Initial investigations were conducted to evaluate the impact of pH and contact time on adsorption. Solutions with varying concentrations of RB ranging from 0.15 to 0.4 mmol dm^{-3} were prepared for this purpose.

3.6. Effect of pH

The investigation into the variation in dye uptake at different pH values involved dispersing approximately 20 mg of each material in a dye solution (10.0 cm^3 of 3.0 mmol dm^{-3}) at a temperature of 298 ± 1 K. After 8 hours, the solutions, with varying pH levels, were analyzed spectrophotometrically at a wavelength of 595 nm. The maximum dye removal occurred at low pH levels (3-6), whereas the minimum dye removal was observed at high pH levels (7-9). Specifically, when the pH was increased to 9, a decrease in dye adsorption was evident, as shown in Fig.(6).

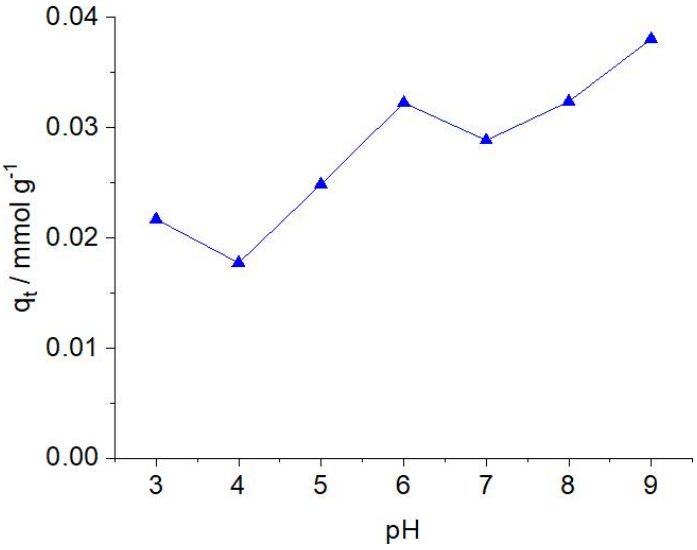

Figure 6. Effect of pH on the sorption capacity of Na-mag for Reactive Blue.

3.7. Kinetic studies

The adsorption capacity of the synthesized Na-magadiite was assessed by investigating the effect of time contact with RB molecules, considering it a reversible reaction at the solid and liquid interface. Adsorption kinetic was conducted by dispersing approximately 15 mg of each material in 10.0 cm^3 of RB solutions at room temperature. At predefined time intervals, samples were analyzed spectrophotometrically at the corresponding λ_{max}. The result of kinetics isotherm is shown in Fig. (7). The dye uptake exhibited a progressive increase with time until reaching a plateau, indicating equilibrium, as depicted in Fig. (6). Equilibrium states were achieved within 150 minutes for NaMG, with no significant difference in adsorption observed beyond this duration. The adsorption kinetics were analyzed using the pseudo-first-order and pseudo-second-order kinetic models [29,30]. The data obtained were fitted to these models to elucidate the dynamics of RB adsorption onto silicates, including order and rate constants. The differential Equation for the pseudo-first-order kinetic model is expressed as Equation (3), while the pseudo-second-order kinetic model is described by Equation (4):

$$\frac{dq_t}{dt} = k_1 (q_e - q_t) \quad (3)$$

$$\frac{dq_t}{dt} = k_2 (q_e - q_t)^2 \quad (4)$$

where

q_e = amounts of dye adsorbed (mg g^{-1}) at equilibrium

q_t = amount of dye adsorbed (mg g^{-1}) at time, t (min)

k_1 = rate constant of pseudo-first-order (min^{-1})

k_2 = rate constant of pseudo-second-order g mg^{-1} min^{-1}.

The correlation coefficients (R^2) obtained from the non-linear fit of the pseudo-first-order and pseudo-second-order models for the adsorption of RB onto NaMG are listed in Table. The rate constant (k1) and equilibrium adsorption capacity (qe) were determined from the plots of log (qe− qt) versus t. The high R^2 values obtained with the pseudo-first-order kinetics suggest that the adsorption of RB onto magadiites follows an ideal pseudo-first-order reaction. The rate constant (k_1) was calculated to be 0.039 min^{-1} for NaMG. Additionally, the calculated qe values using the pseudo-first-order model closely match the experimental values (q_{exp}) (Table), indicating good agreement between the adsorption process and the proposed kinetic model. The lower chi-square value (χ2) further confirms the adequacy of the model in fitting the experimental data.

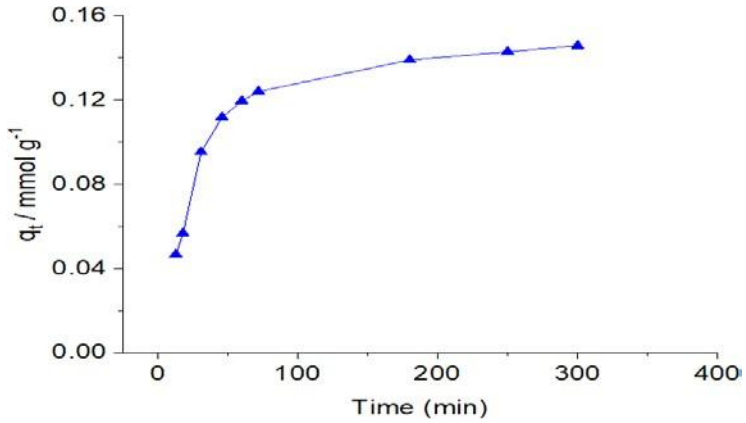

Figure 7. Adsorption isotherms of Reactive Blue on the Na-mag

Table: The pseudo-first-order and pseudo-second-order kinetic models for reactive blue.

Material	$q_{, exp}$ mmol g^{-1}	Pseudo-first-order			Pseudo-second-order		
		q mmol g^{-1}	k_1 min^{-1}	R^2	q_e mmol g^{-1}	k_1 mmol g^{-1} min^{-1}	R^2
Na-Mag	0.021	0.0210±0.01	0.040±0.003	0.99	0.025±0.002	1.800±0.205	0.98

4. CONCLUSION

The Na-magadiite possesses a stable structure with Lewis acidic centers, facilitating stronger interactions with negatively charged dye molecules. Batch-wise adsorption studies have demonstrated the effectiveness of these synthesized materials as efficient adsorbents for the reactive blue (RB) under optimal experimental conditions to achieve equilibrium in aqueous solutions. Kinetic models have shown good agreement between the experimental and expected values. Furthermore, this investigation offers evidence of bonding interactions between the RB dye and the silicate surface. These findings suggest that the synthesized materials are valuable for removing organic waste from water sources.

Acknowledgment:

The authors are thankful to the Institute of Chemistry, University of Campinas, UNICAMP, Campinas, SP, Brazil, for providing research facilities to investigate the present work.

Reference

1. K. Maheshwari, M. Agrawal, A.B. Gupta, *Novel Materials for Dye-containing Wastewater Treatment, Springer Singapore,*1-25**(2021)**.
2. Y. Zhou, J. Lu, Y. Zhou, Y. Liu, *A review, Environ. Pollu*, 252 352-365 **(2019)**
3. A. Mokhtar, S. Abdelkrim, M. Hachemaoui, M. Adjdir, M. Zahraoui, B. Boukoussa, *A review, Appl. Clay Sci*, 198, 105823. **(2020)**
4. J.E. Aguiar, J.A. Cecilia, P.A.S. Tavares, D.C.S. Azevedo, E.R. Castellón, S.M.P. Lucena, *Int.J. Silva, Appl. Clay Sci.,* 135 35-44, **(2017)**
5. D.B. França, S.M. Torres, E.C.S. Filho, M.G. Fonseca, M. Jaber, *Chemosphere*, 222**:** 980-990. **(2019)**
6. K. Ahmed, A.J. Khan, CTGVMT Pires, M. Yamin, F. Rehman, A. Rahim, J. Song, C. Desalination and Water Treatment, 104; 159-168, **(2018)**
7. K. Ahmed, F. Rehman, CTGVMT Pires, A. Rahim, A.L. Santos, C. *Airoldi, Microporous and Mesoporous Mat*., 236 167-175**(2016)**.

8. A.A. Christy, *Colloids and Surfaces A: Physicochem. Engin. Aspects*, 322; 248-252. **(2008)**

9. S.E. Mora-Rodríguez, A. Camacho-Ramírez, J. Cervantes-González, M.A. Vázquez, J.A. Cervantes-Jauregui, A. Feliciano, A. Guerra-Contreras, S. Lagunas-Rivera, *Org. Chem. Front*. 9; 2856-2888. **(2022)**

10. S.A. Jadhav, H.B. Garud, A.H. Patil, G.D. Patil, C.R. Patil, T.D. Dongale, P.S. Patil, Colloid and Interface Sci. Comm. 30; 100181; **(2019)**.

11. M.K. Dinker, P.S. Kulkarni, Recent, J. Chem. & Eng. Data, 60; 2521-2540 **(2015)**

12. M. Delle Piane, M. Corno, P. Ugliengo, *J. Chem. Theory and Computation*, 9; 2404-2415, **(2013)**

13. M. Ge, L. Cao, M. Du, G. Hu, S.M. Jahangir Alam, *Mater. Chem. Phys.,* 217 533-540, **(2018)**

14. G.L. Paz, E.C.O. Munsignatti, H.O. Pastore, *J. Molecular Catalysis A: Chemical*, 422: 43-50. **(2016)**

15. J.L. McAtee, Jr., R. House, HP Eugster, *Magadiite from Trinity County, California, American Mineralogist*, 53: 2061-2069, **(1968)**.

16. H.P. Eugster, *Sci,* 157; 1177-1180 **(1967)**

17. G.B. Superti, E.C. Oliveira, H.O. Pastore, A. Bordo, C. Bisio, L. Marchese, *Chem. Mater*., 19 4300-4315;**(2007)**

18. A. Mokhtar, S. Abdelkrim, A. Djelad, A. Sardi, B. Boukoussa, M. Sassi, A. Bengueddach, *Carbohydrate Polymers*, 229; 115399, **(2020)**

19. M. Zahraoui, A. Mokhtar, B. Fadila, M. Sassi, *J. Inorg. and Organometallic Polymers and Mater.*, 30: 4969-4975. **(2020)**

20. A. Brandt, W. Schwieger, K.H. Bergk, *Crystal Res. Technol.*, 23; 1201-1203, **(1988)**.

21. O.Y. Kwon, K.W. Park, *Bulletin of the Korean Chemical Society*, 25; 25-26, **(2004)**.

22. C.T.G.V.M.T. Pires, N.G. Oliveira, C. Airoldi, *Mater. Chem. Phys*., 135 870-879. **(2012)**

23. B. Royer, N.F. Cardoso, E.C. Lima, T.R. Macedo, C. Airoldi, *Separation Sci.Technl.*, 45**;** 129-141, **(2009)**.

24. C. Eypert-Blaison, E. Sauzéat, M. Pelletier, L.J. Michot, F. Villiéras, B. Humbert, *Chem. Mater*., 13; 1480-1486, **(2001)**

25. CTGVMT Pires, J.R. Costa, C. Airoldi, *Microporous and Mesoporous Materials*, 163; 1-10,**(2012)**.

26. J.S. Dailey, T.J. Pinnavaia, *Chem. Mater*. 4**;** 855-863;**(1992)**.

27. F. Kooli, L. Yan, *J.Phys. Chem*. C, 113; 1947-1952. **(2009)**

28. F. Kooli, L. Mianhui, S.F. Alshahateet, F. Chen, Z. Yinghuai, *J.Phys. Chem Solids,* 67; 926-931**(2006)**.

29. H. Arslanoglu, H.S. Altundogan, F. Tumen, *J. hazard. Mater*., 164; 1406-1413, **(2009)**.

30. YS Ho, G. McKay, *Process Biochem.*, 34 451-465;**(1999)**

Received: February 15th 2024 **Accepted: May 24th 2024**